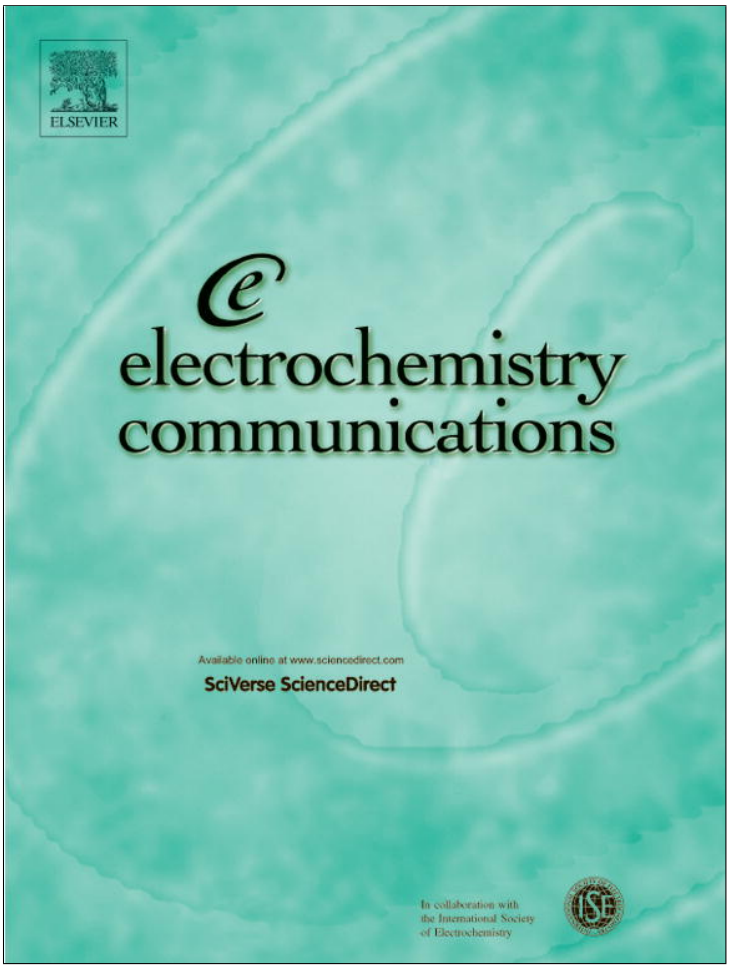

(This is a sample cover image for this issue. The actual cover is not yet available at this time.)

Electrochemistry Communications 21 (2012) 14–17

Contents lists available at SciVerse ScienceDirect

Electrochemistry Communications

journal homepage: www.elsevier.com/locate/elecom

The limits of underpotential deposition in the nanoscale

O.A. Oviedo, L. Reinaudi, E.P.M. Leiva *

Departamento de Matemática y Física, Facultad de Ciencias Químicas, Universidad Nacional de Córdoba, INFIQC, Córdoba X5000HUA, Argentina

ARTICLE INFO

Article history:
Received 18 April 2012
Received in revised form 2 May 2012
Accepted 3 May 2012
Available online 11 May 2012

Keywords:
Underpotential deposition
Nanoparticles
Size control
Nanothermodynamics

ABSTRACT

A thermodynamic model predicting the disappearance of the underpotential deposition phenomenon in the limit of small nanoparticles is proposed and developed for selected families of geometric bodies. The key parameters are the binding energy of adatoms on the flat foreign substrate and at the edges of the nanoparticle.

1. Introduction

Several electrochemical procedures used originally for the modification of planar surfaces are nowadays being successfully applied to NPs [1,2]. Among them, the modification of a metal surface by foreign adatoms using the so-called underpotential deposition (*upd*) phenomenon has shown a great potential for electrochemistry. Surface potential control allows the precise modification of the coverage degree of an adsorbate, even at the submonolayer level [3–5]. The main handicap of this method is probably the fact that it is usually limited to the deposition of a less noble metal on a more noble one. A way to circumvent this problem has been found, producing the galvanic replacement of a sacrificial monolayer previously deposited (*upd*), which shows a larger affinity for the NP [6,7]. Another novel application of *upd* on NPs has been shape control [8]. In these experiments, *upd* is used to block selectively the growth of the material of which the NP is made. By changing the concentration of the metal being deposited, it is possible to obtain NPs of different sizes and shapes [8,9].

In the theoretical field, computer simulations using realistic interatomic potentials showed that the *upd* phenomenon seems to vanish in the Au–Ag [4,10–12] and Pd–Au [13] systems when the size of the substrate (core) is reduced below 2 nm in diameter. Similarly, experiments by Compton and coworkers [14–16] have shown that the *upd* phenomenon vanishes in the nanoscale. There, the *upd* of Pb and Cd on Ag NPs was analyzed at different NP sizes, with the remarkable finding that *upd* is absent for NPs smaller than 70 nm in diameter. As we see, experimental and theoretical evidence shows that the occurrence of this phenomenon may reach a limit for very small NPs. The present work is devoted to discuss one of the reasons why *upd* may vanish in the very small NP limit.

2. Results and discussions

The Gibbs free energy change associated with the formation of a core–shell NP, made of N_{Me} metal atoms of type *Me* adsorbed on a NP constituted of N_S atoms of type *S* can be written as

$$\Delta G(N_{Me},\eta) = \Phi(N_{Me}) + N_{Me} z e_0 \eta \tag{1}$$

where the formation takes place from the bulk material *Me* [4,11] and the naked *S* core, η denotes the overpotential referred to the bulk reversible deposition of *Me*, *z* is the valence of the deposited metal and e_0 is the electronic charge. Although Eq. (1) is formally very similar to the one employed to consider nuclei growth in the classical theory, there are some important differences which were analyzed in detail in different articles by some of us [4,11,12,17]. In the specific case of nanoparticles, Φ contains contribution from the finite size of the system like rotations, translations, etc. [10,11].

For the particular case of the formation of the first monolayer of the foreign material *Me*, we will assume it contains N^*_{Me} atoms, Eq. (1) becomes

$$\Delta G(N^*_{Me},\eta) = \Phi(N^*_{Me}) + N^*_{Me} z e_0 \eta \tag{2}$$

where $\Phi(N^*_{Me})$ may be calculated according to [4]

$$\Phi(N^*_{Me}) = \sum_{i=1}^{m} g^{i}_{Me} N^{i}_{Me} - \mu^{\mathrm{bulk}}_{Me} N^*_{Me} \tag{3}$$

where g^{i}_{Me} corresponds to the free energy of adsorption per atom of *Me* on sites of type *i* on the NP, *m* is an integer denoting the number of site

* Corresponding author: Tel./fax: +54 0351 4344972.
E-mail addresses: ooviedo@fcq.unc.edu.ar (O.A. Oviedo), lreinaudi@fcq.unc.edu.ar (L. Reinaudi), eleiva@fcq.uxnc.edu.ar (E.P.M. Leiva).

1388-2481/$ – see front matter © 2012 Elsevier B.V. All rights reserved.
doi:10.1016/j.elecom.2012.05.001

types (face, edge, corner, etc.) on the NP, N^i_{Me} is the number of adatoms adsorbed on each type of site and μ^{bulk}_{Me} is the chemical potential of the bulk metal *Me*. $\Phi(N^*_{Me})$ depends on core size, as well as on the type of geometry assumed for the core. This dependence will be given by the relative number of adsorption sites on faces, borders, etc., described by the $\{N^i_{Me}\}$ set. These values may be obtained assuming a given geometry (i.e. icosahedral), although it is straightforward to make similar calculations for other geometries.

2.1. Cores with icosahedral geometries

A suitable approximation to study metal deposition on an icosahedral NP with a minimal number of parameters is to assume that it presents only two types of adsorption sites: at the faces and at the edges. Thus, the sum in Eq. (3) is restricted to

$$\Phi(N^*_{Me}) = g^f_{Me}N^f_{Me} + g^e_{Me}N^e_{Me} - \mu^{bulk}_{Me}N^*_{Me} \tag{4}$$

where g^f_{Me} and g^e_{Me} correspond to the adsorption free energy of adatoms at the faces and at the edges of the icosahedron respectively, N^f_{Me} and N^e_{Me} are the corresponding number of adsorption sites, and we have neglected the difference between adsorption free energies at the edges and at the vertices. Fig. 1 (left) illustrates the different adsorption sites.

The consideration of icosahedral geometries allows making a straightforward assignment of N^f_{Me} and N^e_{Me}, which are required to calculate $\Phi(N^*_{Me})$ from Eq. (4). Icosahedra of different sizes are described by an index *n*, which is related to the total number of atoms N_T and the number of atoms at the surface N^*_{Me} through

$$N_T = \frac{1}{3}\left(10n^3 + 15n^2 + 11n + 3\right) \tag{5}$$

and

$$N^*_{Me} = 10n^2 + 2 \tag{6}$$

Thus, the replacement of the numbers $n = 1, 2, 3, \ldots$ into Eqs. (5) and (6) describe icosahedra with a total number of atoms $N_T = 13, 55, 147\ldots$ with $N^*_{Me} = 12, 42, 92\ldots$ atoms at the surface. The number of atoms located at the faces and at the edges can be in turn calculated via

$$N^f_{Me} = 10\left(n^2 - 3n + 2\right) \tag{7a}$$

$$N^e_{Me} = 30n - 18 \tag{7b}$$

respectively. Note that the number of atoms at the faces and at the edges grow quadratically and linearly with *n*, respectively, as physically expected. Using Eqs. (4), (6), (7a), and (7b), and taking into account that $N^*_{Me} = N^f_{Me} + N^e_{Me}$, we get

$$\Phi(N^*_{Me}) = \left(g^f_{Me} - \mu^{bulk}_{Me}\right)N^*_{Me} + \left[30\left(\frac{N^*_{Me}-2}{10}\right)^{1/2} - 18\right]\left(g^e_{Me} - g^f_{Me}\right) \tag{8}$$

Note that the contribution $g^e_{Me} - g^f_{Me}$, which corresponds to the free energy difference between the adsorption an adatom at an edge and the adsorption of an adatom at a facet is a positive quantity, since the latter always exhibits a larger coordination. In contrast, the difference $g^f_{Me} - \mu^{bulk}_{Me}$, which corresponds to the excess of adsorption free energy of an adatom at the (111) facets with respect to the bulk material *Me* may be positive or negative, depending on the strength of the adsorbate–substrate interaction. In a first approximation, if the adsorption free energy on a (111) facet can be approximated by the adsorption free energy on an infinite (111) face, this difference is directly related to the underpotential shift [18–20] on the (111) surface according to $(g^{surf}_{Me} - \mu^{bulk}_{Me}) = -ze_0\Delta E^{upd}_{111}$. With this insight, we can analyze the possibility of *upd* on NPs according to Eq. (8). First of all, it comes out that *upd* on icosahedral NPs is forbidden if this phenomenon does not exist on the infinite (111) surface; Since $g^e_{Me} - g^f_{Me} > 0$ as we analyzed above, $\Phi(N^*_{Me})$ will be greater than zero for all possible N^*_{Me}. If *upd* exists for the infinite (111) surface, the first term on the *rhs* of Eq. (8) will be negative, with the second one remaining positive. While the first term will prevail over the second for large enough N^*_{Me} (relatively large NPs) because of its functional dependence, it may eventually occur that for some (small enough) N^*_{Me}, the second term predominates, resulting in $\Phi(N^*_{Me}) > 0$, thus precluding *upd* on the NP. To go beyond this qualitative analysis, we consider the N^*_{Me} values which are solutions of Eq. (8), say $N^{*,root}_{Me}$ for the case where $\Phi(N^*_{Me}) = 0$. This condition corresponds to the case where the *upd* phenomenon disappears. For N^*_{Me} values smaller than $N^{*,root}_{Me}$ no *upd* should take place. From an experimental point of view, rather than the $N^{*,root}_{Me}$ values, it may be more interesting to know the critical core size below which no *upd* will be found. This may be easily obtained using Eq. (5) to get the total number of atoms in the decorated NP, and subtracting from it $N^{*,root}_{Me}$, we denote this number with N^{root}_S. Fig. 2a shows this critical core size for different combinations of the relevant physical parameters of the model, $-ze_0\Delta E^{upd}_{111} = (g^f_{Me} - \mu^{bulk}_{Me})$ and $(g^e_{Me} - g^f_{Me})$. Fig. 2b shows a similar plot, but with an estimation of the core radius r_{NP} in nanometers, according to $r_{NP}(\text{nm}) = r^0_S(\text{nm})\sqrt[3]{N^{root}_S}$.

Fig. 2 gives an overview of the effect of the relevant physical parameters on the critical NP size for *upd*. For a given system, if the *upd* shift for an infinite surface is known and an estimation of the binding energy of adatoms at an edge and at a face can be made, the critical size can be estimated. Thus, for example, if $ze_0\Delta E^{upd}_{111} = 20$ meV, and

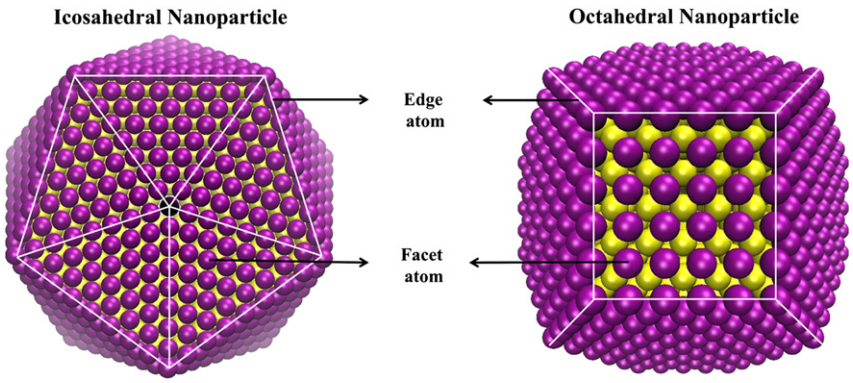

Fig. 1. Different shapes of core–shell nanoparticles modeled in the present work. The yellow spheres correspond to substrate atoms and the purple ones to adatoms. The white lines connect edge adatoms. (For interpretation of the references to color in this figure legend, the reader is referred to the web version of this article.)

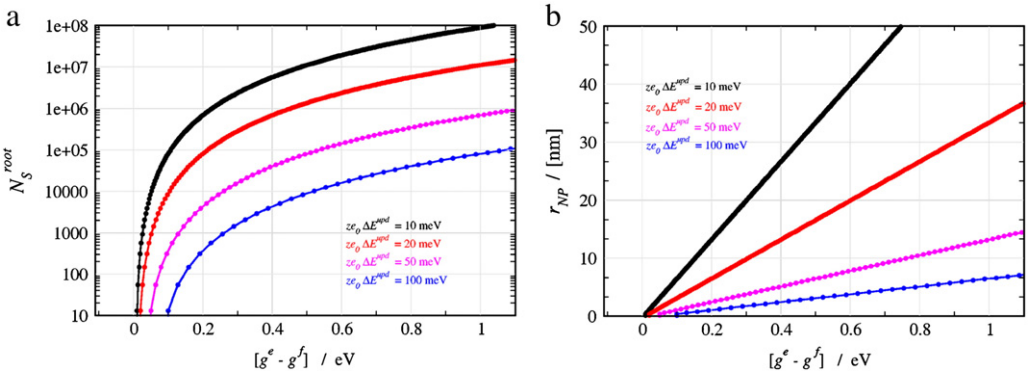

Fig. 2. (a) Critical number of atoms constituting an icosahedral substrate nanoparticle, below which the underpotential deposition phenomenon will vanish, as a function of the difference of adsorption free energies of adatoms at the edges and at the faces ($g^e_{Me} - g^f_{Me}$). Each of the curves corresponds to systems presenting different underpotential shifts on the (111) face, ΔE^{upd}_{111}. (b) shows the same calculations, but reports the ordinates the radius of the substrate nanoparticle r_{NP}. The lines are drawn to guide the eye.

$g^e_{Me} - g^f_{Me} \approx 0.6$ eV, the critical diameter is expected to be of the order of 40 nm.

To get a simple expression for the roots of Eq. (8), if N^*_{Me} is larger than a few hundreds, we can approximate $\{30[(N^*_{Me}-2)/10]^{1/2} - 18\}$ by $\sqrt{90N^*_{Me}}$, resulting in

$$N^{*,root}_{Me} \approx 90\left[\frac{g^e_{Me} - g^f_{Me}}{g^f_{Me} - \mu^{bulk}_{Me}}\right]^2 = 90\left[\frac{g^e_{Me} - g^f_{Me}}{ze_0\Delta E^{upd}_{111}}\right]^2 \quad (9)$$

which indicates that the stronger the *upd* shift, the smaller the particle size at which the *upd* phenomenon will disappear (see Fig. 2). In other words, stronger curvature effects are needed to turn it off when the *upd* phenomenon is strong. It is worth noting here that when using the approximation given in Eq. (9) instead of Eq. (8), the error in $N^{*,root}_{Me}$ is about 6%. This error is acceptable, while Eq. (9) provides simple predictive equation.

Since for metal systems the energetic contribution is the dominant one, we can use in Eq. (9) the energy values calculated in Ref. [21] for Ag adsorption on Au(111) and at the border of a Ag island. Thus, for Ag adsorption on Au(111), we set $g^e_{Ag/Au(111)} \approx -2.76$ eV and $g^f_{Ag/Au(111)} \approx -2.96$ eV, so we can predict the *opd–upd* transition for Ag deposition on Au NPs. The former yields $N^{*,root}_{Ag} \approx 300$ and $N_T \approx 700$ (a NP core with $N^{root}_S \approx 400$). These results can be compared with those of previous computer simulations for the same system [13], where the *opd–upd* transition was found at $N^*_{Ag} \approx 470$. The agreement is particularly good, since in the approximate analysis that we are performing here we only consider two types of adsorption energies, while the computer simulations considered all the many-body interactions.

2.2. Cores with octahedral geometries

Generally speaking, a NP may present different types of facets and borders. This is for example the case of an octahedral core, where the *n*th member of the family fulfills the following relationships:

$$N_T = 16n^3 + 15n^2 + 6n + 1 \quad (10a)$$

$$N^{[100]}_{Me} = 6n^2 - 12n + 6 \quad (10b)$$

$$N^{[111]}_{Me} = 24n^2 - 24n + 8 \quad (10c)$$

$$N^e_{Me} = 36n - 12 \quad (10d)$$

$$N^*_{Me} = 30n^2 + 2 \quad (10e)$$

where $N^{[100]}_{Me}$ and $N^{[111]}_{Me}$ are now the number of atoms at the (100) and (111) facets respectively, and other variables keep their previous meaning. We have also neglected the difference between adsorption free energies at the edges and at the vertices. Fig. 1 (right) shows facet and border atoms in the case of an octahedral NP. Making the approximation $N^*_{Me} - 2 \approx N^*_{Me}$ and after some algebraic work we get for the present case:

$$\Phi(N^*_{Me}) = \frac{N^*_{Me}}{5}\left(4g^{[111]}_{Me} + g^{[100]}_{Me} - 5\mu^{bulk}_{Me}\right) + 6\sqrt{5}\left(N^*_{Me}\right)^{1/2}\left(3g^e_{Me} - g^{100}_{Me} - 2g^{111}_{Me}\right) + 2\left(4g^{111}_{Me} + 3g^{100}_{Me} - 6g^b_{Me} - \mu^{bulk}_{Me}\right) \quad (11)$$

From the roots of this equation we may get as before the critical adsorbate number $N^{*,root}_{Me}$. In the hypothetical case where $g^{100}_{Me} = g^{111}_{Me} = g^f_{Me}$, Eq. (11) reduces to

$$\Phi(N^*_{Me}) = -N^*_{Me}\left(ze_0\Delta E^{upd}_{111}\right) + 18\sqrt{5}\left(N^*_{Me}\right)^{1/2}\left(g^e_{Me} - g^f_{Me}\right) + 2\left(7g^f_{Me} - 6g^e_{Me} - \mu^{bulk}_{Me}\right) \quad (12)$$

With the assumption made concerning the equivalence between the adsorption free energies on (111) and (100) facets, the only difference between Eqs. (12) and (8) is due to the ratio of border to facet atoms. The single fact of changing this ratio shifts the critical NP size to larger values. This is in agreement with results obtained from simulations for the Au(core)–Pd(shell) system, where it was found that the critical NP size is larger for octahedral than for icosahedral NPs [13].

2.3. Other core geometries and "real" nanoparticles

Eqs. (8) and (11) were developed for different families of nanoparticles, with a given geometric shape. Real NPs may present in many cases a much larger number of border sites than those given by the perfect geometries used to model the present system. In these cases, some qualitative considerations can be made on the effect of the relative number of edge to facet sites of the NP. To do that, let us go back to Eq. (3), and let us assume that there are only two types of sites as before to get

$$\Phi(N^*_{Me}) = N^*_{Me}\left[\left(g^f_{Me} - \mu^{bulk}_{Me}\right) + \frac{N^e_{Me}}{N^*_{Me}}\left(g^e_{Me} - g^f_{Me}\right)\right] \quad (13)$$

As we have discussed before, the quantity $(g^f_{Me} - \mu^{bulk}_{Me})$ is always negative if we are dealing with a system presenting *upd* for infinite surfaces, while $(g^e_{Me} - g^f_{Me})$ is a positive quantity, weighted by the ratio N^e_{Me}/N^*_{Me}. This shows that strongly faceted surfaces (large N^e_{Me}/N^*_{Me}) will be more sensitive towards the loss of *upd* upon core size decrease.

3. Conclusion and perspectives

We have taken here the first steps towards the development of a thermodynamic model for the prediction of the limits for underpotential deposition on nanoparticles. It has been found that the *upd* phenomenon vanishes at the nanoscale. We have considered very simple cases, but the model can be extended straightforwardly to more complicated geometries and systems, as long as the geometry of the substrate is known and the binding energy of the foreign adatoms can be estimated for selected adsorption sites. The predictions set only thermodynamics limits to the *upd* phenomenon at the nanoscale. However, kinetic hindrances could of course impose stronger restrictions to *upd*.

Acknowledgments

We acknowledge financial support from CONICET PIP: 112-200801-000983, Secyt Universidad Nacional de Córdoba, Program BID (PICT-BICENTENARIO-2010-123), and PME: 2006-01581.

References

[1] B. Corain, G. Schmid, N. Toshima, Metal Nanoclusters in Catalysis and Materials Science: The Issue of Size Control, Elsevier B. V, 2008.
[2] M.M. Mariscal, S.A. Dassie, Recent Advances in Nanoscience, M. Research Singpost, 2007.
[3] P. Mulvaney, Langmuir 12 (1996) 788.
[4] O.A. Oviedo, E.P.M. Leiva, M.M. Mariscal, Physical Chemistry Chemical Physics 10 (2008) 3561.
[5] O.A. Oviedo, C.F.A. Negre, M.M. Mariscal, C.G. Sánchez, E.P.M. Leiva, Electrochemistry Communications 16 (2012) 1–5.
[6] S.R. Brankovic, J.X. Wang, R.R. Adžic, Surface Science 474 (2001) L173–L179.
[7] S. Park, P. Yang, P. Corredor, M.J. Weaver, Journal of the American Chemical Society 124 (11) (2002) 2428–2429.
[8] M.L. Personick, M.R. Langille, J. Zhang, C.A. Mirkin, Nano Letters 11 (2011) 3394.
[9] T.T. Tran, X. Lu, Journal of Physical Chemistry C 115 (2011) 3638–3645.
[10] O.A. Oviedo, M.M. Mariscal, E.P.M. Leiva, Electrochimica Acta 55 (2010) 8244.
[11] O. A. Oviedo and E. P. M. Leiva, in: M. M. Mariscal, O. A. Oviedo and E. P. M. Leiva (Eds.), Metal Clusters and Nanoalloys: Modeling and Computer Simulation. Springer 2012. In press. ISBN: 978-1-4614-3267-82012.
[12] M. M. Mariscal, O. A. Oviedo and E. P. M. Leiva, Journal of Materials Research (2012) in press.
[13] O. A. Oviedo, L. Reinaudi, M. M. Mariscal and E. P. M. Leiva. Submitted (2012).
[14] F.W. Campbell, Y. Zhou, R.G. Compton, New Journal of Chemistry 34 (2010) 187.
[15] F.W. Campbell, R.G. Compton, International Journal of Electrochemical Science 5 (2010) 407.
[16] Y. Zhou, N.V. Rees, R.G. Compton, ChemPhysChem 12 (2011) 2085.
[17] N.B. Luque, L. Reinaudi, P. Serra, E.P.M. Leiva, Electrochimica Acta 54 (2009) 3011.
[18] W. Schmickler, Chemical Physics 141 (1990) 95.
[19] V. Sudha, M.V. Sangaranarayanan, Journal of Chemical Sciences 117 (2005) 207–218.
[20] E.P.M. Leiva, Electrochimica Acta 41 (1996) 2185.
[21] M. Rojas, Surface Science 569 (2004) 76.